Proceedings of 9th IEEE International Conference
on CYBER Technology in Automation, Control, and Intelligent Systems
July 29- August 2, 2019, Suzhou, China

A Bio-inspired Robotic Fish Fin with Mechanosensation Using Conductive Liquid-Metal-Infused Soft Actuators

Zemin Liu [1], Wenguang Sun [1], Ziyu Ren [3], Kainan Hu[1], Tianmiao Wang [1,2], **Li Wen [1,2]***

***Abstract*—Fish fins not only function as the propeller during swimming but also play an essential role in perceiving the underwater environment. Previous anatomical studies show that the nerves embedded in the fin ray muscles and the membrane. These fin nerves function as the sensory feedback for the swimming of live fishes. Inspired by this feature, we designed and fabricated a multi-material biomimetic fin prototype with sensory capability. Eight typical spiral eGain soft sensors were embedded in the robotic fish fin ray base to mimic the biological fin nerves. This bio-inspired lever-like design could not only respond to robotic fish fin's lateral swing motion but also enhance the fin ray's sensitivity to the external force. The soft actuators with mechanosensation allow the fin to have undulation/folding motions and the capacity of detecting flow disturbance (sensitivity: 0.03m/s water flow). We examined the mechanosensation capability of the prototype in the uniform flow with different velocities and the tilted oncoming flow jet. Through assembling the biomimetic fins to an undulatory robotic fish, we found that the soft fin could sense both the undulatory body motions and the external disturbance (including the strength and direction of the stimuli). This work provides a new approach for robotic underwater sensing over a range of flow speeds and vortex jets and may help to enrich our understanding of the sensory mechanism of live fishes.**

I. Introduction

Biological studies show that the fish fins have a major contribution in producing thrust for swimming and controlling the body balance [1][2]. Recent studies suggest that besides generating forces, another important function of fins is sensing [3]. Noted that many sensory nerves are embedded in the fin membrane [4], the fin base and the inner core of the fin ray [3]. These nerves enable the fins to function as 'flow sensors' [5][6] or even 'touch sensors' in complex aquatic environment [7]. Researchers suggest that the fin system with nerves allow the live fish to sense the external flow perturbation (such as the vortex jet), and is essential for generating motion to maintain the body stability [8]. However, the mechanosensation of the fish fins is still the least understood aspect of fish biomechanics [8].

Previous studies with robotic fins mainly focused on propulsion performance [9]-[14]. However, there are very few reports on the bio-inspired robotic fin with sensory feedback. Hale and her coworkers have developed a robotic pectoral fin with rigid strain resistive sensors on the surface of the fin rays; these sensors can provide bending information of individual fin ray [15]. Due to the limitations of the rigid sensors, this setup cannot be implemented on any flexible robotic fin system with mechanosensation and it is impossible to generate large deformation during locomotion. Recently, soft flow sensor [16], vortex sensor [17] and bio-inspired lateral line flow sensor [18] have been developed for underwater detection. While it is a great challenge to integrate these flow sensors with a flexible robotic fin. To build a bio-inspired flexible robotic fish fin with robust mechanosensation feedback, we need to find the solutions for the following problems. 1) How to develop the soft actuators with soft sensors that can be integrated with flexible robotic fin and have an accurate/tractable dynamic response to the aquatic environment. 2) How to implement a multi-material mechanism that allows fin to behave complex motions including both undulation/folding. 3) How to evaluate the effectiveness of the fin sensory capacities underwater? These issues are challenging and will be investigated in the current study.

In this paper, we presented a bio-inspired robotic fish fin with mechanosensation by using multi-material 3D printing and liquid metal sensing technology. In contrast to previous studies [9][11][15], we applied soft actuation and sensing technologies to the implementation of the robotic fish fin, which can achieve large deformed motions such as erecting/folding and lateral undulation. The skeleton of the robotic fin was printed with multi-materials. An array of fiber-reinforced soft actuators were employed to mimic the inclinator and erector/depressor muscles of fish. Furthermore, we use typical spiral-shaped liquid metal (eGain) soft pressure sensors [19][20] to mimic the sensory nerves. These soft sensors show promising engineering tolerance and dynamic characteristics during our large deformation tests. Based on this sensing technology, we designed several experiments to show the influence of fin ray stiffness on sensing. Through the test of the prototype in both steady and unsteady flows, we demonstrated that our prototype can acquire both the velocity and direction of the flow. Two robotic fins were mounted on the soft median dorsal/anal fin positions of a multi-link robotic fish that can generate biological relevant undulation locomotion. The bio-robotic fin show different responses to the undulatory body phase, amplitude, and frequency, and the feedback signal can potentially be used to infer the robot kinematics. The results from this study could provide a simple and robust approach to enhance the sensing ability of bio-inspired underwater soft robot.

This work was supported in part by National Excellent Youth Science Foundation support projects, China, under contracts 61822303, 61633004, 61333016. Authors are with the School of Mechanical Engineering and Automation [1], Beijing Advanced Innovation Center for Biomedical Engineering [2], Beihang University, Beijing, 100191, People's Republic of China, and Physical Intelligence Department [3], Max Planck Institute for Intelligent Systems, Germany, 70569; please e-mail Prof. Li Wen for contact: liwen@buaa.edu.cn).

978-1-7281-0770-7/19/$31.00 © 2019 IEEE

II. Materials and Methods

A. Design and fabrication of the bio-robotic fish fin

Most teleost fish species can erect or fold their median fins by the erector/depressor muscles [22]**.** To mimic this erect/fold motion of a fish fin (Fig. 1B), we designed a cable driven mechanism that can translate the linear motion of a fiber-reinforced cylindrical soft actuator into fin rays' rotational motion (Fig. 2A). Fin rays were connected by the Kevlar fiber (0.5mm in diameter). The fiber-reinforced cylindrical soft actuator (15mm in diameter, 30mm in length) which was pneumatically activated, was mounted in the bottom of the robotic fish fin to control the fin rays' rotational motion. An elastic tendon was fixed between the first fin ray and the base to generate preload force (0.8N), which made all the fin rays maintain erected (force transmitted through the Kevlar fiber) when the soft bottom actuator was inactive. Biorobotic fish fin was fully erected under the pneumatic pressure of 0kPa (Fig. 2C) and entirely fold down when the soft bottom actuator was pressurized to 291kPa (Fig. 2D).

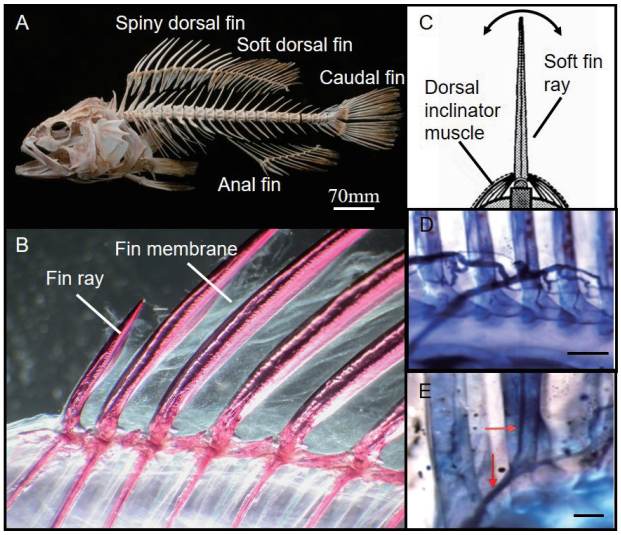

Figure 1. Morphology of the median fins and fin ray structure of bony fishes. (A)The skeleton structure of a snowy grouper (*Hyporthodus niveatus*) showing the vertebral and the major median fins. (B) Image of the dorsal fin in a bluegill sunfish (*Lepomis macrochirus*) to show the rigid fin ray (red) and the soft fin membrane (translucent). (C) Simplified fin ray bending mechanism. Dorsal inclinator muscle can apply force to the base of the fin ray then the fin ray can realize the swing locomotion. (D) also, (E) Sudan black staining of fin nerves (black) [3]. (D) Fin nerves (black) distributes around the fin rays and enters the rays. Scale bar, 1mm. (E) Nerve fibers enter the fin rays at their bases (red arrow) and extend through the core of the ray (red arrow). Scale bar, 0.4mm. [CREDIT: (A), (B) and (C) reprinted from [21], with permission from *Soft Robotics*. (D) and (E) reprinted from [3], with permission from both *Nature Communications* and Hale].

The fin ray of a live fish can be actuated by the dorsal inclinator muscles to achieve the lateral swing motion (Fig. 1B) [23]. Here, two fiber-reinforced cylindrical soft actuators (10mm in diameter, 15mm in length) were placed symmetrically under robotic fin ray's base (Fig. 2B) to mimic the dorsal inclinator muscles. The soft actuator's linear movement could be transferred to the robotic fin ray's lateral swing motion by the joint (inset in Fig. 2B). There are four fin rays in our robotic fin, so four pairs of fiber-reinforced soft actuators were utilized to mimic the dorsal inclinator muscles of four robotic fin rays.

Inspired by the distribution of biological fin nerves, we placed typical liquid metal (eGain) soft pressure sensors between each soft actuator and fin ray's base (Fig. 2B) to mimic the biological fin ray base nerves. This bio-inspired design method made the fin ray mechanism work as a lever system (2-DOF joint was the pivot of the lever system). Fin ray's lever arm is much longer than soft sensor's lever arm, so even a small disturbance imposed on the fin ray or fin membrane would be enlarged to be detected by the soft sensor. The soft pressure sensor's diameter is 10 mm, and the thickness is 2mm. A spiral-shaped microchannel [19][20] was designed to hold liquid metal eGain (Sigma-Aldrich, St. Louis, USA). The dimension of the microchannel is 0.4mmx0.4mm (inset in Fig. 2C).

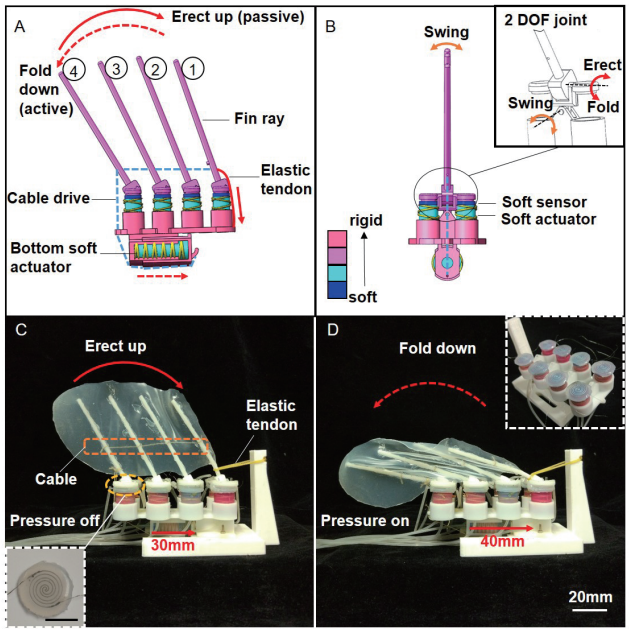

Figure 2. Design of the bio-robotic soft dorsal fin with mechanosensation. (A) and (B) demonstration of the bio-robotic soft dorsal fin's construction. (A) Left view of the three-dimensional model. The bio-robotic soft dorsal fin can mimic the erect up (red arrow) and fold down (dashed red arrow) motion of a biological fish fin. (B) Rear view of the three-dimensional model. Eight small soft actuators were mounted under the fin rays' base. Soft pressure sensor [19][20] was placed between the fin ray base and soft actuator. Inset illustrates the working principle of single fin ray's 2 DOF joint. The orange arrow indicates the swing motion and the red arrow indicates the erect/fold motion. The color bar shows different components' stiffness. (C) Image of an erected bio-robotic soft dorsal fin (the bottom soft actuator is inactive, 30mm in length). Red arrow indicates the erect motion. Inset is a spiral-shaped soft sensor infused with liquid metal, scale bar is 10mm. (D) Image of a folded bio-robotic soft dorsal fin (bottom soft actuator was pressurized to 291kPa, 40mm in length). Red dashed arrow indicates the fold motion. Inset is a robotic fish fin without fin rays and fin membrane.

In this study, soft robotic technology and materials were utilized in the robotic fin's fabrication. The skeleton of the robotic fin was fabricated using 3D printing technology. The material for the fin ray was UV Curable Resin, Young's modulus is 2600MPa. And the material for the base was Polylactic Acid (PLA), Young's modulus is 3300MPa. The multi-step molding process method has been utilized to fabricate the fiber-reinforced soft actuator and the soft sensor [24]. The soft actuator consisted of four components, the inner and outer extendable silicone elastomer layers (Dragon Skin 20; Smooth-on Inc., USA), with Young's modulus of 0.338 MPa. Between the inner layer and outer layer, Kevlar fiber

(0.5mm in diameter) was employed to constrain the radial expansion. Both the driving end (connects with the mechanism) and the fixed end (with a pressure input tube) were sealed with Mold star 30 (Smooth-on Inc., USA), Young's modulus is 0.662 MPa. Ecoflex 00-30 (Smooth-on Inc., USA) was chosen to fabricate the soft sensor, Young's modulus is 0.069 MPa. All the molds were 3D printed using epoxy. The soft fin membrane was manufactured by a spin coater (MV300; Marath, Inc.) using a silicone rubber Ecoflex 00-30 (Smooth-on, Inc., USA). The thickness of the membrane is 700μm. The membrane was glued evenly to the fin rays using silicone epoxy.

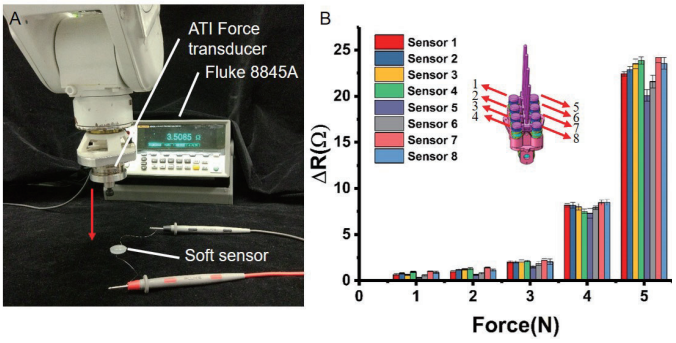

Figure 3. The calibration of the soft sensor. (A) The experimental apparatus for evaluating soft sensor's performance. An ATI force transducer was mounted on the robotic arm to measure the force applied to the soft sensor. The resistance of the soft sensor is acquired by Fluke 8845A. (B) The resistance variation (ΔR) of all soft sensors at different vertical forces (0-5N). The soft sensors' numbers were marked. All the resistance variations are means from n=5 trials.

B. *Experiments on the Force Sensor & robotic fish fin ray*

To evaluate the force sensitivity, we set up an experimental apparatus to calibrate the soft sensors, shown in Fig. 3A. The soft sensor was placed on a horizontal desktop. Eight soft sensors were separately calibrated. The sensor was wired to a precision multimeter (Fluke 8845A, Fluke Inc., USA). A rigid round stamp (9mm in diameter) was utilized to apply force to the soft sensor. To acquire the force applied to the soft sensor, the base of the stamp was fixed to a six-axis force transducer (Mini 40 F/T sensor, ATI, USA). The force transducer was mounted to a robot arm (MOTOMAN MH3F, YASKAWA Inc., Japan) which was programmed to move vertically to generate normal force. To calibrate the soft sensor, the robot arm was programmed to move downward from 0 to 5mm, With a step of 0.1mm. Between two adjacent steps, there was a four-seconds pause. During the process, the resistance data and the force data were recorded simultaneously. Fluke 8845A recorded the resistance, and the NI board recorded the force. Thus we obtained the relationship between the force and resistance. Each trial was repeated for five times.

To evaluate the instantaneous response of the soft sensors. The robotic arm was programmed to push the fin ray tip horizontally at the speed of 5mm/s, 10mm/s, and 50mm/s, shown in Fig.4A. The displacement of the fin ray tip kept 6mm. The soft sensor's resistance was recorded by Fluke 8845A simultaneously during the pushing process. Five trials were conducted to ensure repeatability.

To explore the effect of the fin ray's stiffness on sensing, we designed and fabricated four different stiffness fin rays by changing materials and geometry parameters. These four fin rays are below (arranged in order of stiffness from high to low): PLA fin ray with the diameter of 3.5mm, PLA fin ray with the diameter of 2.5mm, nylon fin ray with the diameter of 3.5mm, nylon fin ray with the diameter of 2.5mm. They are of the same length (80mm). These four fin rays were mounted separately in the single fin ray system (Fig. 4A). The robotic arm was programmed to push these fin rays' tips at the step of 1mm under the same speed 5mm/s; there was a four-second pause between every two steps. The soft pressure sensor's resistance data was recorded by a Fluke 8845A simultaneously.

C. *Experiments on the robotic fish fin*

To demonstrate our bio-robotic fish fin's function as a flow sensor and proprioceptive sensor, we designed four experiments**.** Experiment A and C showed robotic fin's capability in detecting external flow field. Experiment B and D demonstrated robotic fin's function as a proprioceptive sensor to perceive parameters of different fin motions.

To test the robotic fin's sensation of external water flow (in the direction normalize to the fin membrane), the robotic fish fin was fixed on the bottom of the water circulation tank which can generate preciously controlled water flow**.** The direction of the water flow is vertical to the fin membrane (inset in Fig.5A). During the process only the fin-ray three and the corresponding soft senor seven were activated, the resistance was recorded by Fluke 8845A.

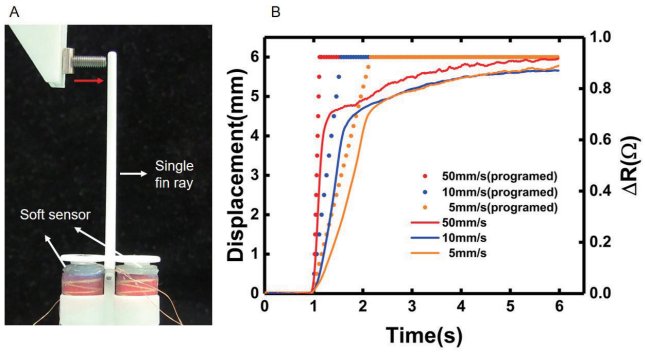

Figure 4. The soft sensor's dynamic response. (A) The experimental apparatus for evaluating the sensor's dynamic response. The robotic arm pushed the fin ray tip horizontally (as the red arrow shows) at a different programmed speed. After horizontal excursion reaching 6mm, the robotic arm held still. (B) The soft sensor's dynamic response at different programmed motion patterns (speed=5mm/s, 10mm/s, 50mm/s). The dotted line represents the robotic arm's programmed displacement, and the dotted line corresponds to the ordinate on the left. The solid line denotes the soft sensor's response, and the solid line corresponds to the ordinate on the right. More details can also refer to the supplementary video section 1.

To demonstrate the robotic fin's proprioception of its movement, we programmed the robotic fin to conduct undulatory motion (the anterior fin rays of a biological fish swing in a minimal amplitude, so we programmed the first fin ray almost still during this experiment). The undulation's period was 2.5s, and the adjacent fin rays' phase difference was 45°. To acquire eight sensors' data simultaneously, we designed a measuring circuit using the differential method. Eight soft sensors were connected in series, and a 50mA current was applied to them. Eight sensors' voltage data was recorded by the NI board simultaneously. According to the soft

sensors' resistance-force calibration data, we could get the force data.

The third experiment was proposed to evaluate the robotic fin's response to an external water flow jet with a tilted angle. During this experiment, the robotic fish fin was fixed in a water tank. A water pump LX-1208 (HeBei LuoXin Inc., China) was employed to produce a tilted oncoming flow jet (original speed is 0.2m/s), the angle between the flow jet and the fin membrane was about 30°. Sensor #1, #2, #3, and sensor #4 were activated in this experiment, so a four-channel measuring circuit using the differential method was proposed to record sensors' data. Simultaneously, the digital particle image velocimetry (DPIV) system (Fig.6A) was utilized to record the flow field generated by the water pump. Moreover, the system includes the laser source, high-speed camera, and particles (10μm average size glass microspheres) to seed the water [25].

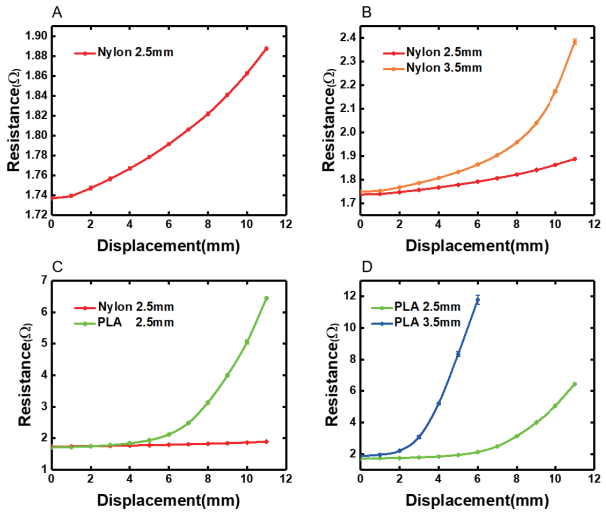

Figure 5. Effect of the fin ray stiffness. The experimental apparatus was shown in figure 4.A. Four different stiffness cylindrical shaped fin rays were fabricated by changing materials (nylon and PLA) and geometry parameters (diameter: 2.5mm and 3.5mm). These fin rays were mounted in a single fin ray system (figure 4.A), and the robotic arm pushed these fin ray tips at the step of 1mm. Soft sensors' response to four fin rays with different stiffness. (A) nylon fin ray with a 2.5mm diameter, (B) nylon fin rays with the diameter of 2.5mm and 3.5mm, (C) nylon fin ray with a 2.5mm diameter and PLA fin ray with a 2.5mm diameter, (D) PLA fin rays with the diameter of 2.5mm and 3.5mm.

To demonstrate the robotic fin's ability to perceive the kinematics of a robotic fish, we mounted the robotic fish fin in a robotic fish (Fig.7A) to test the fin's response to different undulatory frequencies and amplitude**.** The third fin ray and corresponding soft sensors were activated in this experiment. The robotic fish has a body length (BL) of 58.8cm and mass of 2.79kg. The fish body consists of four rigid linkages which can be actuated independently by four servo motors. A serve motor coordinator (MC206; Trio Motion Technology, United Kingdom) controlled these four motors. Thus, we could program the coordinator to generate a fish-like undulatory movement. More details about the robotic fish can be found in our previous work [25][26]. In this experiment, we programmed the robotic fish to move in three motion modes. Motion 1: 1.2Hz in frequency and 0.1 BL in peduncle amplitude. Motion 2: 1.2Hz in frequency and 0.05BL in peduncle amplitude. Motion 3: 0.8Hz in frequency and 0.1BL in peduncle amplitude. Moreover, the flow field of three motion modes was recorded simultaneously by the DPIV system.

III. Results

A. Results of the soft force sensor & robotic fish fin ray

The Fig.3B shows the force-resistance calibration results of the soft sensors. The resistance of the sensor increased as the force increased. The soft sensors showed good repeatability; the error is within ±0.8Ω. (These following experiments' force data was all transferred from soft sensors' resistance data by this force-resistance calibration results).

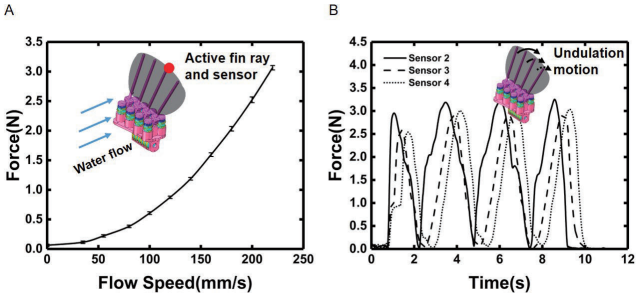

Figure 6. The bio-robotic fish fin's sensation of the external hydrodynamic environment and proprioception of its undulation. (A) The fin sensor's response to different water flow speed. The water flow is vertical to the fin membrane. The red point indicates the active fin ray with sensation. The blue arrow indicates the water flow. (B) The soft sensors' proprioception of the fin rays' undulatory motion in the water.

Fig.4B presents the soft sensor's dynamic response to different pushing speed produced by a robot arm. From this figure, we can see that the sensor's response curve follows the programmed curve very well. During all the pushing velocities (5mm/s, 10mm/s and 50mm/s), the time delays were 0.12s, 0.15s and 0.1s, respectively. Our soft sensor demonstrates a short time delay, which would allow the soft sensors to distinguish small dynamic disturbance. However, due to the soft material's deformation, the sensor takes about 3s to reach steady state after pushing.

Fig.5 provides the experimental data on fin ray stiffness. It is apparent from this figure that fin ray stiffness has a very important influence on the fish fin sensing system. Under the condition that the robotic arm pushed these fin ray tips at the same distance, the higher the fin ray stiffness, the greater the soft sensor output. As the fin ray stiffness increases, the soft sensor is more sensitive to changes in the external environment.

B. Results of the robotic fish fin

Fig.6A illustrates the soft sensor's response to different flow speed. We noticed that the soft sensor's resistance increased as the flow speed increased, a faster water flow applied a more considerable force on the fin membrane. The minimum water flow that the soft sensor can detect is about 30mm/s. This experiment demonstrates the capability of the robotic fish fin can function as a flow sensor.

Fig.6B provides the sensors' proprioception data on robotic fin's undulatory motion. The only difference between the left sensors' output and the right sensors' output was an opposite phase (e.g., the period and frequency of Sensor 2 and Sensor 6 were almost the same, while the phase was opposite).

To make the figure more intuitive, only the left side's sensors' data are provided here. Besides, as the output of sensor 1 was almost a horizontal straight line (the first fin ray swung in a minimal amplitude), so Sensor 1's data is not given here either. It is clear from the figure that the sensing data accurately reproduces the preset key parameters of the undulatory motion. The period (2.5s), phrase difference(45°; Sensor 2's output is ahead of Sensor 3's output 45°, and Sensor 3's output is ahead of Sensor 4's output 45°), and the force produced by the soft actuator can be found in the measured data.

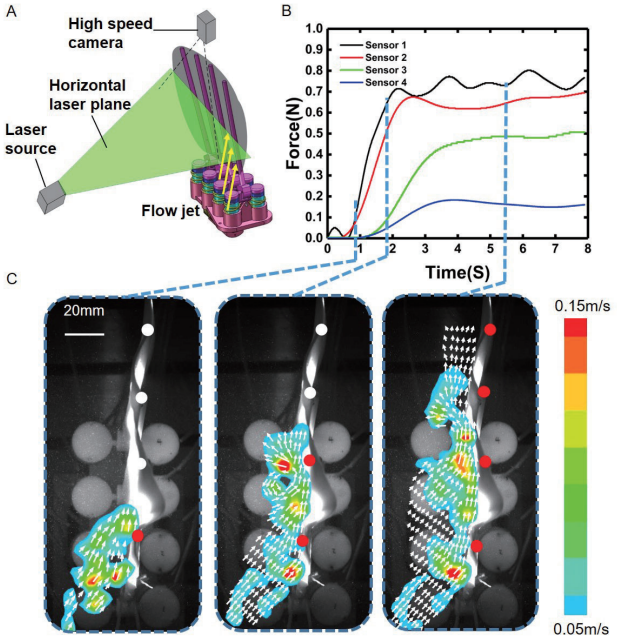

Figure 7. (A) Schematic view of the experimental apparatus. The robotic soft dorsal fin was placed in a water tank. The yellow arrows indicated a tilted flow jet which was generated by a water pump. A high-speed camera was used to record DPIV data, and soft sensors' data was recorded by a DAQ card simultaneously. (B) Soft sensors' response to the tilted flow jet. (C) Time series are illustrating the flow field of the tilted oncoming jet. Circles denote fin ray tip and corresponding soft sensor's positions and current states, red for force and white for no force. The color of the heat map indicates the speed and the arrows indicate the directions of the flow field. Scale bar is 20mm.

Fig.7 shows the robotic fish fin's sensation of a tilted water flow jet. We mimicked the natural external flow disturbance according to a tilted oncoming jet, which principally imposes force on each fin ray. As Fig.6B shows, our sensors output different values as the flow develop along the fin membrane as a function of time. From the response sequence of these sensors, we can know the direction of the flow jet. Sensor 1 first responded to the flow jet and followed by Sensor 2, Sensor 3, and Sensor 4. Therefore, the direction of the flow jet must come from Sensor 1 to Sensor 4. We can also get the direction of the flow jet from the sensors' output value in the stable stage. In the stable stage, Sensor 1 had the largest output value and followed by Sensor 2, Sensor 3, and Sensor 4. It was apparent that the source of the flow jet was closest to Sensor 1, so the direction of the flow jet was from Sensor 1 to Sensor 4. Fig.6C illustrates the flow field overspread trend in time series. We could see the flow field successively imposed force on each fin ray, which corresponds to the response sequence of these sensors. Owing to design restrictions, the current robotic fish fin only perceives the general direction of an external flow jet under the fully open state.

Fig.8 presents sensors' output when the robotic fish performing the undulatory motion. Fig.7C shows the left sensor's (Sensor 7) response to motion 1 (1.2Hz in frequency, 0.1BL in peduncle amplitude) and motion 2 (1.2Hz in frequency, 0.05BL in peduncle amplitude). Fig.7D shows the right sensor's (Sensor 3) response to motion 1 and motion3 (0.8Hz in frequency, 0.1BL in peduncle amplitude). From these two panels, it can be seen that by far the robotic fish fin could accurately distinguish the frequency and amplitude during the undulation. When the robotic fish undulated in 1.2Hz, 0.1 body length (BL) amplitude, the max force acquired by the sensor was 1.2N. During motion 2 and motion 3, the max force were smaller (0.7N and 0.6N). Also, the output's phase of the left sensor and the right sensor was strictly opposite (solid red line in Fig.7C and black solid line in Fig.7D). Combining the relationship between the left and right sensors' outputs, we can obtain the general wave shape of the robotic fish body. Fig.7E and Fig.7F are the flow field correspond to the soft sensor's peak output. The flow field was calculated based on the body-fixed coordinates. Motion 1's flow field's vector length was longer than of motion 2 and motion 3. Flow field data was consistent with sensors' output during different motions.

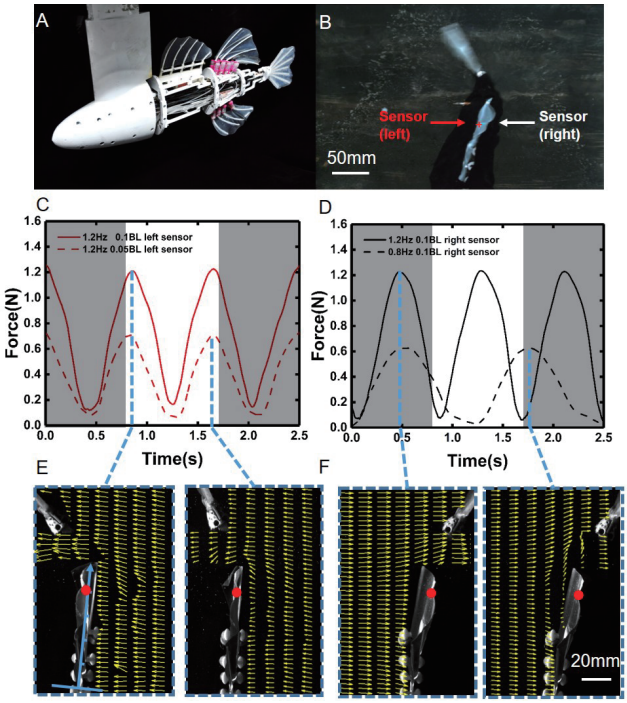

Figure 8. The hydrodynamic experiment for testing the robotic soft dorsal fin's sensing ability. The robotic soft dorsal fin was mounted in a biomimetic robotic fish which can mimic live fish's undulatory locomotion. Undulation frequency and amplitude were under control. (A) Photo of the biomimetic robotic fish with all median fins (BL 580mm). (B) Photo of the robotic fish during the undulation process, the third and corresponding soft sensors were active. (C) Left sensor's (Sensor 7) response to the undulatory locomotion under different peduncle amplitude. Redline is 1.2Hz and 0.1BL, red dashed line is 1.2Hz and 0.05BL. (D) Right sensor's (Sensor 3) response to the undulatory locomotion under different frequency. Blackline is 1.2Hz and 0.1BL; the black dashed line is 0.8Hz and 0.1BL. (E) and (F) are the flow filed corresponds to the soft sensor's peak output. The flow field was calculated based on the blue body-fixed coordinates. Red circle denotes the active fin ray's tip. (E) Flow field corresponds to different undulation amplitude. (F) Flow field corresponds to different undulation frequency. More details can also refer to the supplementary video section 3.

IV. Conclusion and Discussion

In the present work, we demonstrated the design and fabrication of the robotic fish fin, which can sense the flow and mimic the kinematics of its biological counterpart by using soft robotics technology. In general, compared with the traditional robotic fish fin [9][11][12], the significance of the current prototype can be summarized as the following aspects: 1) we applied pneumatic artificial muscles to actuate the fin motions. This approach endows the fin with more flexibility and deformation. 2) This designed prototype can serve as both sensors and actuators. Therefore it enables the sensation of the external hydrodynamic environment and proprioception of its motion. 3) It can sense a large-scale flow and jet.

To mimic the mechanosensation of the biological fin ray, we first applied a two-DOF mechanism for the fin ray (inset in Fig.2B) then, eight small-scale cylindrical soft actuators were positioned symmetrically on both sides of each fin ray. These soft actuators with liquid-metal-infused sensors can not only generate the lateral swing motion but also provide sensory feedback of the force imposed on the fin. Based on the bio-inspired sensory mechanical system, we tested the influence of fin ray stiffness on sensing. Moreover, we found that with the increase of fin ray stiffness, the sensitivity of the sensing system can be improved to some extent. Meanwhile, the erect/fold motion can be realized by the soft actuators which are biologically relevant to the depressor muscle. Having the ability to reduce the fin area (by the erect/fold motion) would further enable the fin working with controllable on/off sensory modes in the confined space.

The soft sensors were placed between each fin ray base and soft actuator. This biomimetic lever-like structural design would promise the robotic fish fin with high sensitivity to the external hydrodynamic environment and proprioception of its own fin ray motion. In the current study, the minimal flow speed that the robotic fin could detect is 0.03m/s. The results also suggest that the soft sensor can accurately acquire the speed of the water flow (vertical to the fin membrane) and identify swimming parameters (phase/ amplitude) of the undulatory motion of the robotic fish. Our robotic fin can also acquire the direction and strength of an external flow jet from the sensors' response sequence. This result can also inspire the future underwater flow sensors includes both strength and direction.

In the future, we will optimize the biomimetic design of the fin ray to further enhance the accuracy and sensitivity of the system.

Acknowledgment

Many thanks to Yufei Hao and Yinglun Jian for their kind help in implementing the experimental apparatus.

References

[1] Lauder, G.V. & Madden, P.G.A. "Fish locomotion: kinematics and hydrodynamics of flexible foil-like fins,". *Experiments in Fluidss*, vol. 43, no. 5, pp. 641–653, Nov. 2007.

[2] Eliot G. Drucker, Lauder, G.V.. "Locomotor function of the dorsal fin in rainbow trout: kinematic patterns and hydrodynamic forces," *Journal of Experimental Biology*, vol. 208, no. 23, pp. 4479-4494, Dec. 2005.

[3] Williams IV, R. et al. "The function of fin rays as proprioceptive sensors in fish," *Nature Communications*, vol. 4, no.1729, Apr. 2013.

[4] Brett R. Aiello et al. "Mechanosensation in an adipose fin," *Proceedings of The Royal Society B*, Vol. 283, no. 1826, Mar. 2016..

[5] T E Reimchen and N F Temple. "Hydrodynamic and phylogenetic aspects of the adipose fin in fishes.," *Canadian Journal of Zoology*, vol. 82, no. 6, pp. 910-916, Jun. 2004.

[6] J. A. Buckland-Nicks, et al. "Neural network detected in a presumed vestigial trait: ultrastructure of the salmonid adipose fin ," *Proceedings of The Royal Society B* , vol. 278, no. 1714, Jul. 2011.

[7] Adam R. Hardy, et al. "Touch sensation by pectoral fins of the catfish Pimelodus pictus," *Proceedings of The Royal Society B* , vol. 283, no. 1824, Feb. 2016.

[8] Richard Williams IV, Melina E. Hale. "Fin ray sensation participates in the generation of normal fin movement in the hovering behavior of the bluegill sunfish (*Lepomis macrochirus*)," *Journal of Experimental Biology*, Vol. 218, no. 21, pp.3435-3447, Nov. 2015.

[9] Tangorra J L, Esposito C J and Lauder, G.V. "Biorobotic fins for investigations of fish locomotion ," in *Intelligent Robots and Systems (IROS), 2009 IEEE/RSJ International Conference on. IEEE*, *2009*, pp2120-2131.

[10] James L. Tangorra et al. "The effect of fin ray flexural rigidity on the propulsive forces generated by a biorobotic fish pectoral fin," *Journal of Experimental Biology*, vol. 213, no. 23, pp.4043-4054. Nov. 2010.

[11] Jonah R. Gottlieb, et al. "A Biologically Derived Pectoral Fin for Yaw Turn Manoeuvres," *Applied Bionics and Biomechanics*, vol. 7, no. 1, pp. 41-55, Dec. 2009.

[12] Rajat Mittal, et al. "Locomotion with flexible propulsors: II. Computational modeling of pectoral fin swimming in sunfish," *Bioinspiration & Biomimetics*, vol. 1, no. 4, pp. 147-162, Dec. 2006.

[13] James L. Tangorra, et al. "The effect of fin ray flexural rigidity on the propulsive forces generated by a biorobotic fish pectoral fin ," *Journal of Experimental Biology*, vol. 213, no. 23, pp. 4043-4054, Nov. 2010.

[14] Ziyu Ren, et al. "Hydrodynamics of a robotic fish tail: effects of the caudal peduncle, fin ray motions and the flow speed A biorobotic model of the sunfish pectoral fin for investigations of fin sensorimotor control," *Bioinspiration & Biomimetics*, vol. 11, no. 1, pp. 411-420, Feb. 2016.

[15] Chris Phelan, et al. "A biorobotic model of the sunfish pectoral fin for investigations of fin sensorimotor control," *Sensors and Actuators A: Physical Bioinspiration & Biomimetics*, vol. 5, no. 3, pp. 349-356, Aug. 2010.

[16] Zhiyuan Liu, et al. "3D-Structured Stretchable Strain Sensors for Out-of-Plane Force Detection." *Advanced Materials*, vol. 30, no. 26, Jun, 2018

[17] Jahan Zeb Gul, et al. "Fully 3D Printed Multi-Material Soft Bio-Inspired Whisker Sensor for Underwater-Induced Vortex Detection," *Soft Robotics*, vol. 5, no. 2, Apr. 2018.

[18] Zhifang Fan, et al, "Design and fabrication of artificial lateral line flow sensors" *Journal of Micromechanics and Microengineering*, vol.12, no. 5, Jun. 2002.

[19] Y-L. Park, , Bor-Rong Chen, and R J. Wood. "Design and fabrication of soft artificial skin using embedded microchannels and liquid conductors." *IEEE Sensors journal,* pp2711-2718, Dec.2012

[20] Y.-L. Park, B. Chen, and R. J. Wood, "Soft artificial skin with multimodal sensing capability using embedded liquid conductors," in *Proc.IEEE Sensors Conf.*, Limerick, Ireland, Oct. 2011, pp. 1–3.

[21] Li Wen, et al. "Understanding Fish Linear Acceleration Using an Undulatory Biorobotic Model with Soft Fluidic Elastomer Actuated Morphing Median Fins," *Soft Robotics*, vol. 5, no. 4, Aug. 2018.

[22] B. C. Jayne, Lauder, G.V. "Speed effects on midline kinematics during steady undulatory swimming of largemouth bass, Micropterus salmoides," *Journal of Experimental Biology*, vol. 198, no.2, pp. 585-602, Feb. 1995.

[23] Silas Alben, et al, "The mechanics of active fin-shape control in ray-finned fishes," *Journal of The Royal Society Interface*, vol. 4, no. 13, Apr. 2007.

[24] Park Y L, et al. "Design and Fabrication of Soft Artificial Skin Using Embedded Microchannels and Liquid Conductor," *IEEE Sensors Journal*, vol. 12, no. 8, pp. 2711-2718, Aug. 2012.

[25] Li Wen, et al. "Novel Method for the Modeling and Control Investigation of Efficient Swimming for Robotic Fish," *IEEE Transactions on Industrial Electronics*, Vol. 59, no. 8, pp. 3176-3188, Aug. 2012,.

[26] Li Wen, et al. "Quantitative Thrust Efficiency of a Self-Propulsive Robotic Fish: Experimental Method and Hydrodynamic Investigation," *IEEE/ASME Transactions on Mechatronics*, vol. 18, no. 3, pp.1027-1038, Jun. 2013.